PHYSICAL REVIEW E **74**, 036103 (2006)

Reaction-diffusion fronts in systems with concentration-dependent diffusivities

Piotr Polanowski[1] and Zbigniew Koza[2]
[1]*Department of Molecular Physics, Technical University of Łódź, Żeromskiego 116, 90-924 Łódź, Poland*
[2]*Institute of Theoretical Physics, University of Wrocław, M. Borna 9, 50203 Wrocław, Poland*
(Received 23 March 2006; published 5 September 2006)

We examine properties of a reaction front that forms in irreversible reaction-diffusion systems with concentration-dependent diffusivities. We study two different models of such systems and find that in the limit of a vanishingly small diffusivity of the reaction product, the reaction front dynamics enters a separate universality class, with the front width asymptotically tending to a constant value, and the reaction rate at the reaction front center diminishing with time t as $t^{-1/2}$. This behavior can be also observed in systems with nonvanishing (but small) diffusivity of the reaction product at intermediate times.

DOI: 10.1103/PhysRevE.74.036103 PACS number(s): 82.20.−w, 68.35.Fx, 66.30.Ny

I. INTRODUCTION

Reactions at the phase boundary play an important role in many industrial and biological processes. Their characteristic feature is formation of a reaction front between initially separated reactants [1–5]. This phenomenon controls the reaction kinetics and can be described in the simplest way as follows: initially two kinds of species (say, A and B) are separated by an impenetrable barrier. The barrier is removed at time $t=0$ and the reactants start to form the reaction front. The reactant species mix before they react if their mobility is fast enough in comparison with their reactivity. This leads to a series of different kinetic regimes between the initial and the asymptotic long-time behavior.

The simplest model of an irreversible reaction diffusion process ($A+B\rightarrow 2C$, where C denotes an inert product), is based on four assumptions. First, the diffusion is the only transport mechanism and the diffusion coefficients D_A, D_B, and D_C of each species are strictly constant, i.e., independent of spatial location, reactant concentrations, etc. Second, the concentrations a, b, and c of species A, B, and C, respectively, effectively depend on time t and only one space coordinate x (even though the system is three dimensional), and their evolution is governed by the reaction-diffusion equations [6],

$$\frac{\partial a(x,t)}{\partial t} = D_A\frac{\partial^2 a(x,t)}{\partial x^2} - R(x,t), \tag{1}$$

$$\frac{\partial b(x,t)}{\partial t} = D_B\frac{\partial^2 b(x,t)}{\partial x^2} - R(x,t), \tag{2}$$

$$\frac{\partial c(x,t)}{\partial t} = D_C\frac{\partial^2 c(x,t)}{\partial x^2} + 2R(x,t), \tag{3}$$

where $R(x,t)$ is the local reaction rate. Third,

$$R(x,t) = ka(x,t)b(x,t), \tag{4}$$

where k is the microscopic reaction rate. Fourth, species A and B are initially separated along the x axis,

$$a(x,0) = a_0H(-x), \quad b(x,0) = b_0H(x), \quad c(x,0) = 0, \tag{5}$$

where a_0 and b_0 are the initial concentrations of species A and B, respectively, and $H(x)$ is the Heaviside step function (which is 0 for $x<0$ and 1 for $x>0$).

Besides $R(x,t)$, the dynamic properties of the reaction-diffusion front at a macroscopic level can be described with the help of the total reaction rate

$$R(t) = \int_{-\infty}^{\infty} R(x,t)dx, \tag{6}$$

the position of the center of reaction front $x_f(t)$ [defined as the point at which $x_f(x,t)$ attains its maximum value], the width of the reaction front

$$w^2(t) = \int_{-\infty}^{\infty} [x - x_f(t)]^2\frac{R(x,t)}{R(t)}dx, \tag{7}$$

and the height of the front $h(t)=R(x_f(t),t)$ [6].

This relatively simple system exhibits many interesting features. Using a scaling ansatz, Galfi and Rácz [6] showed that $w(t)$ grows asymptotically as t^{α} with a surprisingly small value of the exponent $\alpha=1/6$. It was then argued that Eq. (4) can be used for systems with the space dimensionality $d \geqslant 2$, whereas for strictly one-dimensional systems not only $\alpha\neq 1/6$, but also the mean-field approximation (4) breaks down and the fluctuations of reactant concentrations must be taken into account [7–10]. It was also shown [11–13] that the case where one of the reactants is immobile ($D_A=0$ or $D_B=0$) belongs to a separate, "universality class," with $\alpha=0$. The reaction front was found to be mobile under certain conditions [6,11], and even able to change the direction of its motion [14,15]. The quasistatic approximation [8,16] was used to find a detailed description of concentrations of species A, B, and C outside the reaction zone [12,17,18] and the case of equal diffusion coefficient was treated rigorously [19]. These theoretical results are in full agreement with experiments [20–26].

The approach based on Eqs. (1)–(5) assumes strictly constant values of the diffusion coefficients of all species (independent of spatial location and concentrations of reactants and products). Correlations of motion between A, B (substrates), and C (product) species is completely neglected, which is reflected by the fact that Eqs. (1) and (2) depend neither on c nor D_C and can be solved independently of Eq. (3). However, in many real systems (especially in those with high concentrations of A and B) the diffusivities of the substrates and of the product are not constant, but depend on the local concentrations of A, B, and C. Examples of processes with concentration-dependent diffusivities include surface diffusion [27], diffusion in polymers [28,29] and colloidal suspensions [30], diffusion of $CuSO_4$ solution in pure water [31], diffusion in porous [32,33] and nanoporous [34] materials, and interdiffusion in alloys [35]. The aim of this paper is to study a particular case of a reaction-diffusion front in a system with concentration-dependent diffusivities.

The structure of the paper is as follows. In Sec. II we define two models: a macroscopic (mean-field) system of reaction-diffusion equations with concentration-dependent diffusivities and a microscopic model based on the dynamic lattice liquid (DLL) model. Sec. III presents analysis of these models. This includes a discussion of consequences of a scaling ansatz for the macroscopic model and numerical solutions of the two models considered. The main result is that reaction-diffusion systems with concentration-dependent diffusivities can switch to a separate universality class if the diffusivity of the reaction product is much smaller than that of the substrates. Section IV is devoted to conclusions.

II. MODELS

A. Macroscopic mean-field reaction-diffusion equations

Consider a three-dimensional system of reaction-diffusion partial differential equations

$$\frac{\partial a}{\partial t} = \nabla(D_A \nabla a) - kab,$$

$$\frac{\partial b}{\partial t} = \nabla(D_B \nabla b) - kab,$$

$$\frac{\partial c}{\partial t} = \nabla(D_C \nabla c) + 2kab, \tag{8}$$

where a, b, c are the local concentrations of substrates A, B, and the product C, respectively, and D_A, D_B, D_C are the local diffusion coefficients for the substrates and the product, respectively. We assume that initially there is no product in the system and the species A and B are segregated along the $x=0$ plane,

$$a(x,y,z;t=0) = a_0 H(-x),$$

$$b(x,y,z;t=0) = b_0 H(x),$$

$$c(x,y,z;t=0) = 0, \tag{9}$$

where $H(x)$ is the Heaviside step function.

To predict general properties of the solutions to the system (8) with the initial condition (9) is a formidable task. To make the problem more tractable mathematically, we make a few simplifying assumptions. First, we assume that all diffusion coefficients are the same functions of concentrations, i.e., $D_A = D_B = D_C \equiv D(a,b,c)$. Second, we assume that D is linear in relative concentrations of A, B, and C, i.e.,

$$D = \frac{D_A^* a + D_B^* b + D_C^* c}{a + b + c}, \tag{10}$$

where D_X^*, $X = A,B,C$, denotes the diffusion coefficient of species X in the "pure" system filled only with this species. Third, we assume that both the diffusivities of the substrates and their initial concentrations are the same ($D_A^* \equiv D_B^*$, $a_0 = b_0$).

Let $\rho \equiv a+b+c$ denote the cumulative concentration of all species. By summing up all equations in Eq. (8), we arrive at

$$\frac{\partial \rho}{\partial t} = \nabla(D \nabla \rho).$$

Since initially $\nabla\rho = 0$, we conclude that $\rho(x,y,z,t) = a_0$ for all x, y, z, and t. Moreover, as initially the local concentrations of A, B, and C are independent of y and z, they will remain y and z independent for all times. We can thus assume that a, b, and c depend only on x and t. The mathematics involved in the problem can be simplified further by measuring length, time, and concentration in units of $\sqrt{D_A/ka_0}$, $1/ka_0$, and a_0, respectively [36], which leads to $k=1$, $D_A^* = D_B^* = 1$, and $a_0 = b_0 = 1$. With all these simplifications, our original problem reduces to solving

$$\frac{\partial a(x,t)}{\partial t} = \frac{\partial}{\partial x}\left((a + b + D_C^* c)\frac{\partial a}{\partial x}\right) - ab, \tag{11}$$

$$\frac{\partial b(x,t)}{\partial t} = \frac{\partial}{\partial x}\left((a + b + D_C^* c)\frac{\partial b}{\partial x}\right) - ab, \tag{12}$$

$$c(x,t) = 1 - a - b \tag{13}$$

with the initial condition

$$a(x,0) = H(-x), \quad b(x,0) = H(x), \quad c(x,0) = 0. \tag{14}$$

All these simplifications result in an effectively one-dimensional system of reaction-diffusion partial differential equations with only one free parameter D_C^*. Owing to the system symmetry, the reaction front center is fixed at $x_f = 0$ for all t.

B. Microscopic model

To study the problem on the microscopic level, we use the dynamic lattice liquid (DLL) model [37,38]. This model is based on the concept of strictly cooperative motion of molecules in a dense system. As depicted in Fig. 1, the cooperative rearrangements on the lattice have a form of closed loops of displacements of at least three molecules. In contrast to many other lattice models, the DLL model allows one to study lattice systems with the density factor $\rho = 1$ (i.e., with all lattice sites occupied) with full and easy control of mobilities of different species on the microscopic level. Moreover, its properties are in good agreement with dynamical properties of liquids [39,40].

In our simulations we employ a triangular lattice, with periodic boundary conditions along the y axis, and confined

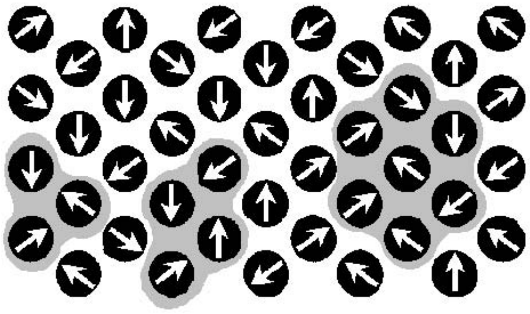

FIG. 1. An example of the vector field that defines directions of attempted molecular displacements toward neighboring lattice sites in the DLL model. Shadowed groups represent closed loops of at least three molecules; only displacements in these groups will actually take place.

between two neutral, impenetrable walls along the x axis. Time is assumed to be a discrete variable and positions of all molecules are updated simultaneously. At any moment each lattice node is occupied by exactly one molecule (of type A, B, or C), and to each molecule k a unit vector $\mathbf{v}_k$ is assigned that points randomly at one of the nearest neighbor sites. This vector represents the direction along which the molecule attempts to jump to an adjacent site. At the beginning of each time step the conditions for the reaction to occur are verified: for each A (B) molecule a neighboring site is randomly chosen and if it is occupied by B (A) then the reaction $A+B\to 2C$ occurs with a given probability p. Next, a new vector field $\{\mathbf{v}_k\}$ is randomly assigned to the molecules. Then all closed loops determined by these vectors are identified. Those molecules that do not belong to a closed loop consisting of at least three molecules are immobilized at this time step. For the molecules that form a loop, a probability π of making a concerted displacement is calculated as the product $(\pi_A)^{n_A}(\pi_B)^{n_B}(\pi_C)^{n_C}$, where n_A, n_B, n_C are the numbers of molecules of type A, B, C (respectively) in the loop, and π_A, π_B, π_C are parameters from the interval [0, 1] that control the mobility of species A, B, and C, respectively. We assume that the mobilities of species A and B are the same and greater than that of species C—hence, for numerical efficiency, we set $\pi_A=\pi_b=1$. Consequently, the microscopic model has two free parameters, π_C and p. The former is closely related to the diffusion coefficient D_C, and the latter corresponds to the reaction rate k. The influence of π_C on the self-diffusion constant for several planar and three-dimensional lattices was analyzed in Ref. [39].

It should be noticed that the microscopic model is significantly different from the macroscopic one defined in Sec. II A. Not only does it take into account correlations between motions of individual molecules, but also exhibits a different dependency of the diffusivities on the concentrations. In particular, in the macroscopic model the local mobilities of all species are assumed to be the same, whereas in the DLL model they are independent of each other.

III. RESULTS

A. Scaling analysis

Consider the long-time limit solutions of Eqs. (11)–(14). Following Refs. [6,17], where the case of constant diffusion coefficients was investigated, we assume that the asymptotic solutions we are looking for can be described with two scaling relations satisfied in two overlapping ranges of x that span the whole system.

The first region is located in the vicinity of the reaction front center $x_f=0$. In this region Eqs. (11) and (12) describe a balance between the reaction-induced loss of particles A, B, and their influx caused by diffusion. The scaling ansatz in this region takes on the form [6]

$$a(x,t) \approx t^{-\beta/2} S_A(x/t^{\alpha}), \quad |x| \lesssim t^{\alpha}, \tag{15}$$

$$b(x,t) \approx t^{-\beta/2} S_B(x/t^{\alpha}), \quad |x| \lesssim t^{\alpha}, \tag{16}$$

where $\alpha \geqslant 0$, and $\beta \geqslant 0$ are some scaling exponents, and S_A, S_B are the scaling functions for a and b in the first region.

The second scaling region is located far from the reaction front, where the reaction term is negligible, and the scaling is valid only for the substrate with higher concentration. The scaling ansatz in this region takes on the form [17]

$$a(x,t) \approx t^{-\nu} s_A(x/t^{\phi}), \quad x \lesssim -t^{\alpha}, \tag{17}$$

$$b(x,t) \approx t^{-\nu} s_B(x/t^{\phi}), \quad x \gtrsim t^{\alpha} \tag{18}$$

with some exponents $\nu \geqslant 0$, $\phi \geqslant 0$ and the scaling functions s_A, s_B for a and b. As $\lim_{x\to-\infty} a(x,t) = \lim_{x\to\infty} b(x,t)=1$, we immediately get

$$\nu = 0. \tag{19}$$

B. The case $D_C^*=0$

Upon assuming $D_C^*=0$ and inserting the first scaling ansatz (15), (16) into the reaction-diffusion equations (11), (12) we find that at $x=x_f=0$ the reaction term $ab \propto t^{-\beta}$, and the diffusion terms $\nabla(D\nabla a)$, $\nabla(D\nabla b) \propto t^{-\beta-2\alpha}$. In the reaction front region the two terms must be balanced, which implies

$$\alpha = 0. \tag{20}$$

On the one hand, the total number of particles B that have reacted till time t can be estimated as $I(t) \approx \int_{x=x_f}^{\infty} [1 - b(x,t)]dx$. Using Eq. (18) we arrive at $I(t) \approx t^{\phi}$ in the limit of $t \to \infty$. On the other hand, $I(t)$ can be calculated as $\int_{\tau=0}^{t} R(t)d\tau$. Using Eqs. (15), (16) we can estimate

$$R(t) \propto t^{\alpha-\beta}, \tag{21}$$

to find that $I(t) \approx t^{1+\alpha-\beta}$ for $t \to \infty$. Taking into account Eq. (20) and comparing the two expressions for the asymptotic behavior of $I(t)$ we arrive at

$$\phi = 1 - \beta. \tag{22}$$

The diffusion term $\nabla(D\nabla a)$ is positive near the reaction front (the first region) and negative far from the reaction front (the second region), so it must vanish at some $\tilde{x}_A(t)$. At this point the concentration of B is much smaller than that of A, and so $D \approx a$. Upon solving the equation

$$\frac{\partial}{\partial x}\left(a(x,t)\frac{\partial a(x,t)}{\partial x}\right)\bigg|_{x=\tilde{x}_A(t)} = 0$$

we find that

$$a(x,t) \approx \sqrt{-f(t)x + g(t)}, \quad \text{for } x \approx \tilde{x}_A(t), \tag{23}$$

where $f(t)$ and $g(t)$ are some functions. If we assume that in the vicinity of $\tilde{x}_A(t)$ both scaling relations for the substrate A, i.e., Eq. (17) and (15) are valid [17], and express Eq. (23) in the forms predicted by the scaling relations, we arrive at $\beta = \phi$ and

$$a(x,t) \propto \sqrt{x/t^{\phi}}, \quad \text{for } x \approx \tilde{x}_A(t), \quad t \to \infty. \tag{24}$$

Using Eq. (22) we finally get

$$\beta = \phi = 1/2. \tag{25}$$

Thus for $D_C^*=0$, the scaling exponents α, β, ν, and ϕ assume the same values as in the case of the $A+B$ (static) $\to 0$ reaction-diffusion system with immobile species B and constant mobility of species A [11–13]. However, all the scaling functions (s_A, s_B, S_A, and S_B) are different in these two cases. This conclusion can be justified in several ways. First, the $A+B$ (static)$\to 0$ system is asymmetric about the (time-dependent) reaction front center $x_f(t)$, while the system studied here is symmetric about $x_f=0$ [i.e., $s_A(x)=s_B(-x)$, $S_A(x)=S_B(-x)$]. Second, in the $A+B$ (static)$\to 0$ reaction-diffusion problem, relation Eq. (24), which settles the boundary conditions for all the scaling functions, has a completely different form, $a(x,t) \propto x/t^{1/2}$ [12,13].

C. The case $D_C^* \neq 0$

In the limit of a large time t and in the vicinity of $x=0$ the concentrations of A and B tend to 0 and so $c=1-a-b$ goes to 1. Consequently, the diffusion constant D in Eq. (10) tends to D_C^*. Therefore if $D_C^* \neq 0$, the asymptotic behavior of the reaction front is effectively governed by

$$\frac{\partial a}{\partial t} = D_C^* \frac{\partial^2 a}{\partial x^2} - ab, \tag{26}$$

$$\frac{\partial b}{\partial t} = D_C^* \frac{\partial^2 b}{\partial x^2} - ab, \tag{27}$$

i.e., by the standard reaction-diffusion equations studied already by Galfi and Racz [6]. The asymptotic ($t \to \infty$) values of the exponents are thus given by

$$\alpha = 1/6, \quad \beta = 2/3, \quad \phi = 1/2. \tag{28}$$

D. Numerical solution of the mean-field model

To verify the predictions of the scaling ansatz, we solved Eqs. (11)–(14) numerically for several values of D_C^*. The value of the exponent α can be conveniently calculated from analysis of the reaction front width $w(t)$, which, as implied by Eqs. (15) and (16), should asymptotically grow as t^{α}. This quantity, calculated for $D_C^*=0$, 0.01, 0.1, and 1, is shown in Fig. 2. For short times t, $w(t)$ is independent of D_C^* and grows as $t^{1/2}$, which implies $\alpha \approx 1/2$, in accord with predictions of Ref. [14]. However, for larger times $w(t)$ starts to depend on D_C^*. In particular, for $D_C^*=1$ our results show that at large times $w(t) \propto t^{\alpha}$ with $\alpha \approx 0.1667$, in excellent agreement with the theoretical value 1/6 predicted in Eq. (28). On the other hand, for $D_C^*=0$ we obtained $\alpha \approx 0$, in accord with Eq. (20). For D_C^* close to 0 the behavior of $w(t)$ first resembles that typical of the case $D_C^*=0$ (with $\alpha \approx 0$) and only for very large t does it switch to the behavior predicted by Eq. (28), e.g., $\alpha = 1/6$.

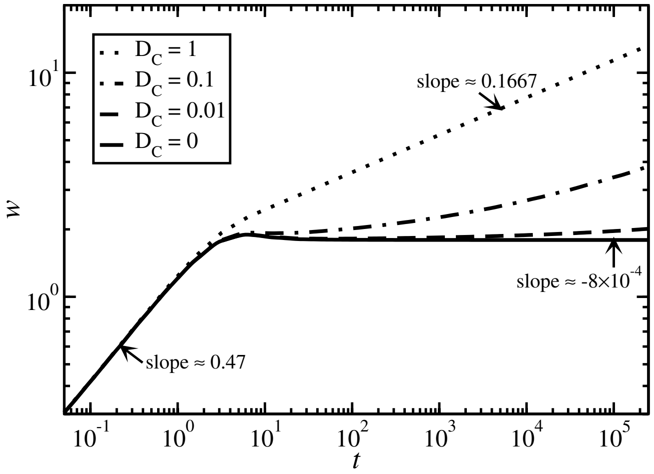

FIG. 2. Width of the reaction front w as a function of time t calculated numerically for $D_C^*=1$, 0.1, 0.01, and 0 (arbitrary units).

Equations (15) and (16) imply that for large times t the concentration of species A (or B) at $x=x_f$ should tend to 0 as $t^{-\beta/2}$. Therefore in Fig. 3 we show a log-log plot of $a(x_f,t)$ obtained for several values of D_C^*, since the slope of the curves in this plot can be identified with $-\beta/2$. For $D_C^*=0$ (solid line) the slope at $t \approx 10^4$ is ≈ -0.2505, in good agreement with Eq. (25). Our analysis predicts that for all nonzero values of D_C^* the slope should asymptotically tend to $-1/3$.

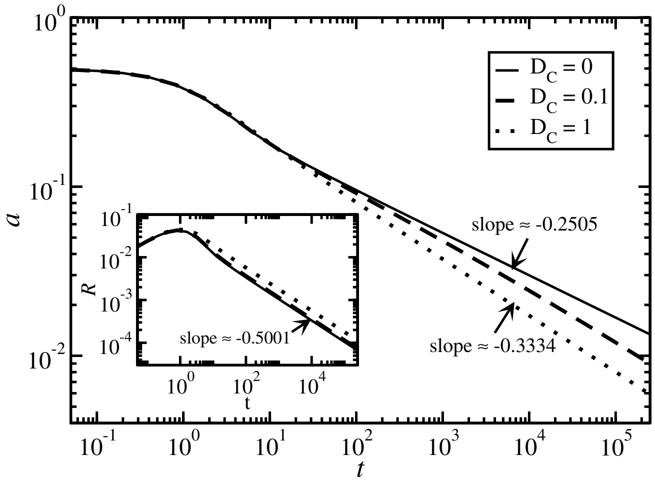

FIG. 3. Temporal evolution of the concentration of species A at $x=x_f$ for $D_C^*=0$, 0.1, and 1. Inset: the total reaction rate $R(t)$ for the same values of D_C^* (arbitrary units).

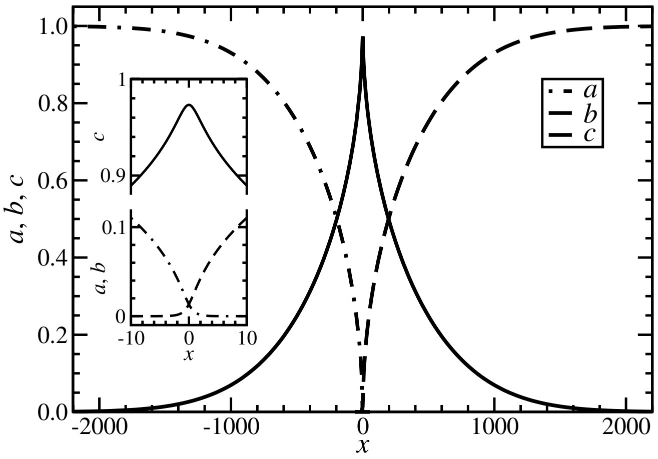

FIG. 4. Concentration of species A, B, and C at $t=2.5\times 10^5$ for $D_C^*=0$ (arbitrary units). In this case the diffusion coefficient $D=a+b$ and at $x=0$ it goes to 0 as $t\to\infty$. Inset: enlargement of the region $x\approx 0$.

This is confirmed by the results obtained for $D_C^*=1$ (dotted line), for which the slope is close to $-1/3$ as early as at $t=10$. For $D_C^*=0.1$ the slope also tends to $-1/3$, although not as fast as for $D_C^*=1$.

An interesting and somewhat surprising consequence of the scaling analysis is that the total reaction rate $R(t)$ should asymptotically decrease as $t^{\alpha-\beta}=t^{-1/2}$ irrespective of D_C^*. Since the diffusivity near x_f tends to D_C^*, one could naively expect that for $D_C^*=0$ the diffusion of species A and B through the reaction front region will be eventually blocked, which should result in a rapid decrease of $R(t)$ at large t. However, as illustrated by the inset in Fig. 3, the asymptotic behavior of $R(t)\propto t^{-1/2}$ is the same whether D_C^* vanishes or not; actually the asymptotic reaction rate for $D_C^*=1$ turns out only $\approx$70% higher than that for $D_C^*=0$.

To explain this property, in Fig. 4 we have plotted the concentration profiles of species A, B, and C obtained for the case $D_C^*=0$. The current of species A entering the reaction zone is $j_A=|D\nabla a|\approx a|\nabla a|$. Using Eq. (24) we obtain $j_A\propto t^{-\phi}=t^{-1/2}$. Thus the blocking effect of a vanishingly small diffusivity $D=a+b$ near $x=0$ (which goes to 0 as $t^{-1/4}$) is compensated by diverging gradients ∇a and ∇b of species A and B.

E. Simulations of the microscopic model

As it was explained in Sec. II B, the microscopic model has two free parameters, $p,\pi_C\in[0,1]$, with p controlling the reaction rate, and π_C corresponding (in a complicated, nonlinear way) to the mobility of species C. We performed simulations of the model using various combinations of these parameters, with p ranging from 0.0001 to 0.005 and $\pi_C=0$, 0.1, 0.25, and 1.

Our first finding was that except for the case of immobile C ($\pi_C=0$), the local reaction rate $R(x,t)$ turns out proportional to the product of the local concentrations of species A and B, i.e., $R(x,t)\propto a(x,t)b(x,t)$. This implies that for $\pi_C>0$ the model belongs to the class of the systems whose evolution can be described by reaction-diffusion equations (8). However, in contrast to the macroscopic model of Sec. II A, the dependence of the diffusion coefficients D_A, D_B, and D_C in Eq. (8) on the local concentrations a, b, and c is not known explicitly. In particular, D_A, D_B, and D_C are all different, probably nonlinear functions of a, b, and c.

For $\pi_C=0$, the reaction product is immobile and one can expect that it will quickly form an impenetrable barrier for the species A and B. The reaction rate will rapidly go to 0 even though the product ab remains nonzero inside the barrier area. This implies that the mean-field equations (8) cannot be used if the reaction product is immobile—this case must be considered separately.

The next step is to reduce the number of relevant parameters in the model. Recall that in the macroscopic model this was achieved by making use of dimensional analysis. However, application of this method in the microscopic model is not straightforward, as its control parameters p and π_C are (dimensionless) probabilities. This difficulty can be overcome by noticing that for sufficiently small values of the reaction probability p, this parameter is proportional to the reaction rate k in Eq. (8). Since one can eliminate k in Eq. (8) by measuring length and time in units of $k^{-1/2}$ and k^{-1}, respectively, we can expect a similar simplification if length and time in the microscopic model are measured in units of $p^{-1/2}$ and p^{-1}, respectively. All our data, collected for various values of p, confirm this conjecture. This implies that the only relevant control parameter of the model is π_C.

We start our simulations from setting $\pi_C=1$, which corresponds to a system with concentration-independent diffusion coefficients. This well-known case was already studied by Galfi and Rácz and many researchers who followed their pioneering paper [6], and we use it as a test case for the validity of the computer code. Then we investigate systems with reduced π_C, i.e., the case where the diffusion coefficients are concentration dependent, and focus on the limit of $\pi_C\to 0$, for which our theory of Sec. II B predicts a different universality class. Finally, we check the behavior of the system for the singular value of $\pi_C=0$.

The temporal evolution of the reaction front width $w'=w\sqrt{p}$ for several values of p and π_C is depicted in Fig. 5. As can be seen, for times $\tau=tp\lesssim 1$, the width w satisfies the scaling law $w(\tau)\propto\sqrt{\tau}$ of Taitelbaum *et al.* [14] for reaction-diffusion fronts at short times. The physical interpretation of this result is that initially the effect of the reaction is negligible compared to that of diffusion, so the system evolves as if the species A and B did not interact with each other. For times $\tau\gtrsim 1$ the situation becomes more interesting. On the one hand, for $\pi_C=1$ the reaction front width quickly assumes the asymptotic behavior predicted by Galfi and Rácz [6], i.e., $w(\tau)\propto\tau^{1/6}$. On the other hand, for $D_C<1$ the width develops a clear maximum at $\tau\approx 2$. Moreover, for large times and $\pi_C\to 0$, there is a time interval where $w(t)$ assumes practically a constant value, in accord with our predictions and numerical results in Secs. III B and III D. For larger times the value of $d\ln w/d\ln\tau$ starts to increase and we conjecture that in the limit of $\tau\to\infty$ the with $w(\tau)$ will be proportional to $t^{1/6}$ for all $\pi_C>0$.

Figure 6 shows the temporal evolution of the (dimensionless) total reaction rate $R'=R/\sqrt{p}$ for several values of π_C

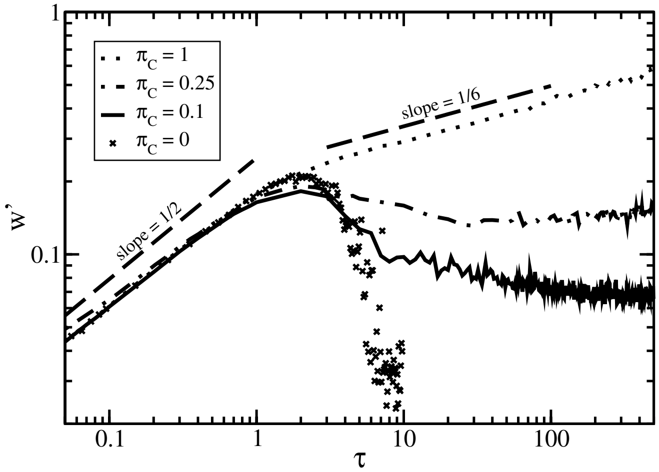

FIG. 5. The dimensionless width $w'=w\sqrt{p}$ as a function of dimensionless time $\tau=tp$ calculated in the microscopic model for $(\pi_C,p)=(1,0.001)$, (0.25, 0.005), (0.1, 0.0001), and (0, 0.0001).

and p. As should be expected [14], initially $R'(\tau)$ is independent of π_C and p, and for $\pi_C=1$ the total reaction rate diminishes to 0 as $\tau^{-1/2}$. However, for $\pi_C \ll 1$ one can identify a region of intermediate times where $R'(\tau)$ decays far more quickly than $\tau^{-1/2}$. This region is visible particularly well in the singular case where the product is immobile ($\pi_C=0$); actually in this case $R'(\tau)$ decays as rapidly as τ^{-3}. We attribute this unexpectedly quick decay to the blocking effect of the C species that form in the reaction front region and inhibit the reaction. The blocking persists till the time τ' such that the diffusion length $\sqrt{\pi_C\tau'}$ is comparable in magnitude with the reaction front width $w(\tau')$. For times $\tau \gg \tau'$, R' decays as τ^{η}. However, while for $\pi_C=1$ the numerical estimation of $\eta \approx -0.51$ is close to the theoretical value $\eta=-1/2$ obtained in Ref. [6] for the limit of $\tau \to \infty$, the agreement for $\pi_C=0.25$ and $\pi_C=0.1$ is not as good. In particular, we estimate $\eta \approx -0.39$ for $\pi_C=0.25$ and $\eta=-0.44$ for $\pi_C=0.1$. These values indicate that the system has not reached the long-time limit regime. This statement can be justified as follows: since diffusion is the only transport mechanism, $\int_{t=0}^{\tau} R'(t)dt$ is bounded from above by a term proportional to $\tau^{1/2}$, hence η must be $\leqslant -0.5$ in the long-time limit.

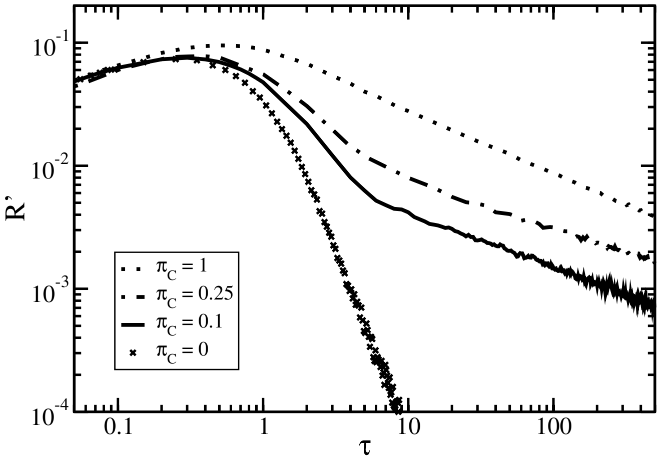

FIG. 6. The dimensionless total reaction rate $R'=R/\sqrt{p}$ as a function of dimensionless time $\tau=tp$ for the same values of π_C and p as in Fig. 5.

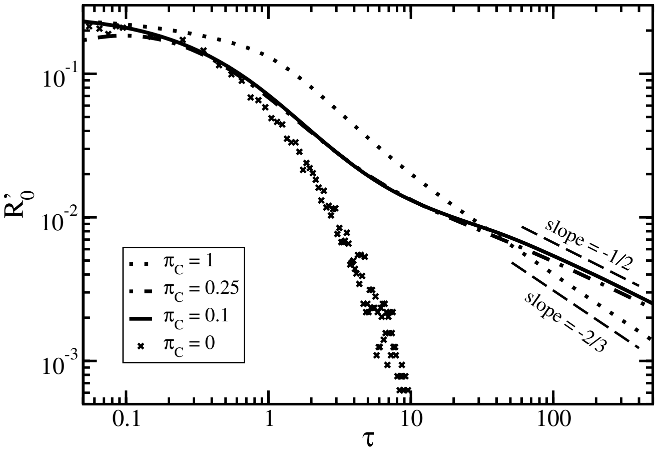

FIG. 7. The dimensionless reaction rate at the reaction front center, $R_0'(\tau)=R(0,t)/p$ as a function of dimensionless time $\tau=tp$. The simulation parameters are the same as in Figs. 5 and 6.

Finally, in Fig. 7, we present the evolution of the rescaled reaction rate $R_0'(\tau)=R(0,t)/p$. For $\pi_C=1$ the long-time behavior of this quantity is in agreement with the mean-field theory of Galfi and Rácz, who predicted that $R_0'(\tau)\propto\tau^{-\beta}$ with $\beta=2/3$ [6]. However, $\beta\approx 1/2$ for $\pi_C=0.25$ and $\pi_C=0.1$, in accord with our prediction (25) for the limit of $D_C \to 0$.

As we have noted, the case $\pi_C=0$ is singular, as in this case the immobile reaction product forms an impenetrable barrier that renders the mean-field approximation (4) invalid. For this reason this case constitutes a separate "universality class," with very rapid and probably nonuniversal decay of the reaction rate.

IV. SUMMARY AND OUTLOOK

Our study shows that evolution of reaction fronts in systems with concentration-dependent diffusivities exhibits a rich variety of kinetic behaviors. In particular, when the diffusivity of the reaction product is much smaller than that of the substrates, the system can go through four distinct kinetic regimes characterized by exponents α and β that control the width w and height h of the reaction front, respectively [$w(t)\propto t^{\alpha}$, $h(t)\propto t^{-\beta}$], and exponent η that controls the total reaction rate R [$R(t)\propto t^{\eta}$]. In the first kinetic regime, which is typical of all initially separated reaction diffusion systems, the reaction kinetics is determined solely by diffusion; this regime is characterized by $\alpha=1/2$, $\beta=0$, $\eta=1/2$ [14]. In the second kinetic regime the reaction is inhibited by almost immobile reaction product that has quickly built in the reaction front area during the initial stage of the process. In this kinetic regime, which is actually a short-lived transient rather than a well-defined scaling regime, $\alpha<0$ (the reaction front shrinks) and $\eta<-1/2$. In the third kinetic regime the evolution is still determined by a very small diffusivity of the reaction product; however, reaction is not blocked, for the substrates and the product can diffusively mix in the reaction front region and their small mobility is compensated by large gradients of the substrate concentrations. In this kinetic regime $\alpha \approx 0$ (the reaction width does not change) and $\beta \approx 1/2$. The fourth, asymptotic kinetic regime is typical of all irreversible reaction-diffusion fronts in systems with nonvanishing diffusivities in the large-time limit. It is characterized by Galfi's and Rácz's exponents $\alpha = 1/6$, $\beta = 2/3$, and $\eta = -1/2$. Transition to this kinetic regime turns out very slow, probably because it requires reconstruction of not only the concentration profiles inside the relatively narrow reaction layer, but also outside it, on a distance proportional to the width of the depletion zone for species A and B, i.e., on a distance $\propto \sqrt{t}$. This reconstruction is necessary to establish the proper boundary conditions for the concentration profiles inside the reaction front.

A natural question arises to what extent our results are general. For example, the second kinetic regime does not appear in our macroscopic model based on differential equations. This, however, is explained by the fact that in this model the diffusivities of all species are assumed to be locally the same, so no blocking effect is possible. In most real situations an excess of the reaction product in the reaction front should inhibit the reaction, so the second kinetic regime should be a common property of most reaction-diffusion systems with concentration-dependent diffusivities. As to the third kinetic regime, it should be common to all systems where the diffusivity of the reaction product is much smaller than that of the substrates. However, further work is necessary to determine whether the values of the exponents $\alpha \approx 0$ and $\beta \approx 1/2$ are universal or if they are system dependent. Another interesting problem is to examine the reaction-diffusion fronts with concentration-dependent diffusivities in more complex systems, e.g., in nonsymmetric systems (with $a_0 \neq b_0$ or $D_A \neq D_B$) or in systems with a reversible reaction. Of course it would be of highest interest to verify our conjectures experimentally.

ACKNOWLEDGMENT

This work was partially supported by KBN Grant No. 3 T08A 018 26 (Poland).

---

[1] D. Avnir and M. Kagan, Nature (London) **307**, 717 (1984).

[2] G. T. Dee, Phys. Rev. Lett. **57**, 275 (1986).

[3] H. K. Henisch, *Periodic Precipitation* (Pergamon, Oxford, 1991), Vol. 57.

[4] S. A. Rice, *Diffusion Limited Reactions* (Elsevier, Amsterdam, 1985).

[5] D. ben Avraham and S. Havlin, *Diffusion and Reactions in Fractals and Disordered Systems* (Cambridge University Press, Cambridge, England, 2000).

[6] L. Galfi and Z. Rácz, Phys. Rev. A **38**, R3151 (1988).

[7] B. P. Lee and J. Cardy, Phys. Rev. E **50**, R3287 (1994).

[8] S. Cornell and M. Droz, Phys. Rev. Lett. **70**, 3824 (1993).

[9] P. L. Krapivsky, Phys. Rev. E **51**, 4774 (1995).

[10] S. J. Cornell, Phys. Rev. E **51**, 4055 (1995).

[11] Z. Jiang and C. Ebner, Phys. Rev. A **42**, 7483 (1990).

[12] Z. Koza, Physica A **240**, 622 (1997).

[13] M. Z. Bazant and H. A. Stone, Physica D **147**, 95 (2000).

[14] H. Taitelbaum, S. Havlin, J. E. Kiefer, B. Trus, and G. H. Weiss, J. Stat. Phys. **65**, 873 (1991).

[15] Z. Koza and H. Taitelbaum, Phys. Rev. E **54**, R1040 (1996).

[16] E. Ben-Naim and S. Redner, J. Phys. A **25**, L575 (1992).

[17] Z. Koza, J. Stat. Phys. **85**, 179 (1996).

[18] M. Sinder and J. Pelleg, Phys. Rev. E **61**, 4935 (2000).

[19] A. Schenkel, P. Wittwer, and J. Stubbe, Physica D **69**, 135 (1993).

[20] Y.-E. L. Koo and R. Kopelman, J. Stat. Phys. **65**, 893 (1991).

[21] H. Taitelbaum, Yong-Eun Lee Koo, S. Havlin, R. Kopelman, and G. H. Weiss, Phys. Rev. A **46**, 2151 (1992).

[22] A. Yen, Yong-Eun Lee Koo, and R. Kopelman, Phys. Rev. E **54**, 2447 (1996).

[23] H. Taitelbaum, B. Vilensky, A. Lin, A. Yen, Yong-Eun Lee Koo, and R. Kopelman, Phys. Rev. Lett. **77**, 1640 (1996).

[24] S. H. Park, S. Parus, R. Kopelman, and H. Taitelbaum, Phys. Rev. E **64**, 055102(R) (2001).

[25] C. Leger, F. Argoul, and M. Z. Bazant, J. Phys. Chem. B **103**, 5841 (1999).

[26] C. N. Baroud, F. Okkels, L. Ménétrier, and P. Tabeling, Phys. Rev. E **67**, 060104(R) (2003).

[27] J. V. Barth, Surf. Sci. Rep. **40**, 75 (2000).

[28] G. D. J. Phillies, in *Statistics of Linear Polymers in Disordered Media*, edited by B. Chakrabarti (Elsevier, Burlington, MA, 2005), pp. 305–356.

[29] F. Müler-Plathe, Chem. Phys. Lett. **252**, 419 (1996).

[30] Z. Chvoj, J. M. Lahtinen, and T. Ala-Nissila, J. Stat. Mech.: Theory Exp. 2004 P11005.

[31] M. Küntz and P. Lavallée, J. Phys. D **37**, L5 (2004).

[32] L. Pel, K. Kopinga, G. Bertram, and G. Lang, J. Phys. D **28**, 675 (1996).

[33] A. E.-G. E. Abd and J. J. Milczarek, J. Phys. D **37**, 2305 (2004).

[34] S.-S. Chong, H. Jobic, M. Plazanet, and D. S. Sholl, Chem. Phys. Lett. **408**, 157 (2005).

[35] R. Filipek, J. Mol. Liq. **86**, 69 (2004).

[36] B. Chopard, M. Droz, T. Karapiperis, and Z. Rácz, Phys. Rev. E **47**, R40 (1993).

[37] T. Pakula, J. Mol. Liq. **86**, 109 (2000).

[38] P. Polanowski and T. Pakula, J. Chem. Phys. **117**, 4022 (2002).

[39] P. Polanowski and T. Pakula, J. Chem. Phys. **118**, 11139 (2003).

[40] P. Polanowski and T. Pakula, J. Chem. Phys. **120**, 6306 (2004).